



New Enaminone Derivatives of 6-Hydroxy-4,7-dimethoxy-benzofuran-5-yl Scaffold: Synthesis, Antimicrobial and Antioxidant Activities, and Molecular Docking Studies as Potential DNA Gyrase B and DHFR Inhibitors



CrossMark

Ashraf A. Sediek^{1*}, Shaima A. El-Mowafi², Ahmed Younis³, Mohamed S. Abdel-Aziz⁴, Eman Sabry¹

¹Chemical Industries Institute, National Research Centre, 12622 Dokki, Giza, Egypt;

²Peptide Chemistry Department, National Research Centre, 12622 Dokki, Giza, Egypt;

³Green Chemistry Department, Chemical Industries Institute, National Research Centre, 33 El Bohouth st. (former EL Tahrir st.)-Dokki-Giza- P.O.12622, Egypt.

⁴Microbial Chemistry Department, Biotechnology Research Institute, National Research Centre, 12622 Dokki, Giza, Egypt.

Abstract

A new series of enaminone derivatives of 6-hydroxy-4,7-dimethoxy-benzofuran scaffold have been synthesized using a simple and practical coupling reaction of enaminone **2** with different primary amines to give benzofuran derivatives **3a-j**. The same enaminone was allowed to interact with different hydrazone derivatives **4a-d** to yield the corresponding pyrazole derivatives **5a-d**. All derivatives were characterized with IR, ¹H NMR and ¹³C NMR techniques. The antimicrobial activity of the new compounds was determined for Gram-positive and Gram-negative bacterial strains using agar well diffusion method. The MIC assay was then assessed. Further *in vitro* assays showed that **3g** moderately inhibited DNA gyrase, while **5b** weakly inhibited DNA gyrase. Additionally, both compounds **3g** and **5b** moderately inhibited DHFR *in vitro*. Compound **3g** was shown to be able to form stable complexes with both DNA gyrase and DHFR, as demonstrated by the docking studies. All compounds except **3e** presented a prominent total antioxidant activity

Keywords: Khellin; Benzofuran; Antimicrobial; Antioxidant; Molecular docking; DNA gyrase; DHFR

1. Introduction

Through the hybridization of several pharmacophores, many biologically active compounds have recently been created and presented as novel entities with anticipated therapeutic actions [1]. Although the pharmacophores may serve as the biological activity center, hybridization is anticipated to amplify the biological impact of two pharmacophores with comparable activities [1-3]. Numerous of these potent hybrid compounds are presently undergoing various stages of clinical trials [4]. Heterocyclic compounds are an important part of the main components of natural compounds and are utilized in pharmaceutical and therapeutic applications [5,6]. Benzofuran and its derivatives are predominant heterocyclic compounds and represent the backbone substrate for many natural compounds [7-9]. With a fused benzene and furan ring, benzofuran is an oxygen-containing heterocycle with a variety of biological characteristics. The first benzofuran-based molecule was isolated from the ancient arab medicinal plant khella (khellin and visnagin) which carried the benzofuran and chromium skeletons together [10]. Many relevant compounds containing the benzofuran moiety have been isolated from natural sources, which have shown effectiveness in various medical applications [11,12]. Benzofuran and its derivatives showed a broad spectrum of substantial biological activities including antimicrobial [13,14], antifungal [15,16], antiviral, antitubercular [17], antioxidant [18,19], anti-inflammatory [20,21], anticonvulsant [22], analgesic [21], antipyretic, anticancer [13], anti-Alzheimer's [23], and selective enzyme inhibitory activities [18,23,24]. Therefore, the wide range of biological activities associated with this versatile scaffold has led the benzofuran moiety to be considered for hybridization with other heterocycles to produce novel compounds with enhanced biological efficacy [25-28]. Hybrid derivatives, which combine the benzofuran moiety with other pharmacophores, have shown promise in improving drug efficacy and reducing resistance [8,29-32]. The current research work focuses on the synthesis of benzofuran-based hybrid derivatives with antimicrobial and antioxidant activities. The growing concern over microbial resistance and the increasing need for effective antioxidants have intensified research into novel bioactive compounds. Indeed, antibiotic resistance is regarded as one of the most prominent global health issues. A recent 2023 WHO report warned of an upcoming era with no antibiotics available to treat common secondary bacterial infections because of a cumulative increase in the number of pathogens resistant to antimicrobial drugs [33]. Targeting microbial resistance can be performed by targeting crucial bacterial events, such as DNA replication and biosynthesis of tetrahydro folic acid (THF) [34]. DNA gyrase is a type II topoisomerase essential for relaxation of supercoiled DNA, which is required for bacterial DNA replication [35,36]. Inhibition of DNA gyrase results in inhibition of cell division

*Corresponding author e-mail: aa.sediek@nrc.sci.eg; (Ashraf A. Sediek).

Received date 28 September 2024; Revised date 21 October 2024; Accepted date 27 October 2024

DOI: 10.21608/ejchem.2024.324405.10532

©2025 National Information and Documentation Center (NIDOC)

and bacterial cell death [35,36]. On the other hand, dihydrofolate reductase enzyme (DHFR) is essential for folate metabolism and synthesis of purines and pyrimidines required in bacterial cell proliferation [37]. Consequently, the development of novel benzofuran-based derivatives as antimicrobial agents with the potential to inhibit bacteria by different mechanisms such as inhibiting DNA gyrase and DHFR represents a proper target to face the challenge of antimicrobial resistance. These derivatives can exhibit a broad spectrum of antimicrobial activity against both Gram-positive and Gram-negative bacteria, as well as fungi [38]. Additionally, their antioxidant properties help in mitigating oxidative stress, which is implicated in numerous chronic diseases [29]. The synthesis and biological assessment of benzofuran derivatives from enaminones have only been documented in few articles. The chemical complexity and bioactivity of these derivatives are increased when enaminones are incorporated into benzofuran structures, which makes them promising candidates for therapeutic development. For instance, Sanad et. al study discusses the synthesis and applications of a novel enaminone derivative incorporating a dibromobenzofuran moiety. This enaminone acted as a precursor for the synthesis of novel imino derivatives, azines and azolotriazines [39]. Another paper discusses the synthesis of a bis(benzofuran-enaminone) hybrid with a piperazine linker, along with its use as a precursor for the synthesis of bis (pyrido [2',3':3,4] pyrazolo[1,5-a]pyrimidines) by microwave-assisted methods. The study highlighted the efficiency of this method, involving coupling the enaminone precursor with various diazonium salts and yielding novel heterocyclic compounds with potential biological applications [40]. As a continuation of our studies on physiologically active heterocycles, new hybrid compounds based on benzofuran were created and their antioxidant and antibacterial properties assessed. The most potent substances were then tested for their ability to block the DHFR enzyme and E. Coli DNA gyrase. To have a deeper understanding of the biological outcomes acquired, *in silico* experiments were conducted and thoroughly analyzed.

2. Experimental

Chemistry

All reagents and solvents were of commercial grade. Khellin (Chemical Industries Development Company, El Omraniya, Giza, Egypt). Melting points were measured on the digital melting point apparatus (Electro thermal 9100, Electro thermal Engineering Ltd, serial No. 8694, Rochford, United Kingdom) and are uncorrected. The reaction progress was monitored by thin layer chromatography (TLC) using aluminum sheets silica gel 60 F254 (Merck). Elemental analyses were carried out on a Perkin-Elmer 2400 analyzer (USA), and were found within ± 0.4 % of the theoretical values. FT-IR spectra were recorded on a Bruker spectrometer (Bruker Tensor 27, Tokyo). Mass spectra were recorded on a Shimadzu EIMS spectrometer (GCMS-QP 1000 EX, 70 Ev). ¹H and ¹³C NMR spectra were measured with a Bruker model (300 MHz) Ultra Shield NMR spectrometer in DMSO-d₆ using tetramethylsilane (TMS) as an internal standard. 1-(6-Hydroxy-4,7-dimethoxybenzofuran-5-yl) ethan-1-one (1) [41] and (E)-3-(dimethylamino)-1-(6-hydroxy-4,7-dimethoxybenzofuran-5-yl)prop-2-en-1-one (2) [42,43] were prepared as previously reported.

General Synthesis of compounds 3a-j

Twenty-nine milligrams of enaminone 2 (10 mmol) and several amino-compounds (aniline, 4-substituted anilines [4-Me, 4-Br, and 4-Cl], benzyl amine, sulfanilamide, sulfadimidine, 2-aminobenzimidazole, 6-aminocoumarin, and furfurylamine) (10 mmol) in (20 mL) of absolute ethanol containing (1 mL) of glacial acetic acid were refluxed for 3-7h under follow-up of TLC. After the reaction ended, it was concentrated to half its volume. The precipitate formed was filtered and recrystallized from the proper solvent.

1-(6-Hydroxy-4,7-dimethoxybenzofuran-5-yl)-3-(phenylamino) prop-2-en-1-one (3a). yellow powder, MP 144-6 °C (MeOH); yield 60%. The IR (KBr, cm⁻¹) ν 3500 (OH), 3102 (NH), 1702 (C=O). ¹H NMR (300 MHz, DMSO-d₆) δ 12.83 (s, 1H), 10.27 – 10.25 (d, J = 6 Hz, 1H), 8.17 – 8.11 (t, J = 9 Hz, 1H), 7.87 - 7.86 (d, J = 3 Hz, 1H), 7.39 – 7.31 (m, 3H), 7.13 – 7.10 (dd, J = 6, 3 Hz, 2H), 7.05 – 7.04 (d, J = 3 Hz, 1H), 6.55 – 6.53 (d, J = 6 Hz, 1H), 3.98 (s, 3H, OCH₃), 3.94 (s, 3H, OCH₃). ¹³C NMR (75 MHz, DMSO-d₆) δ 185.7, 154.6, 152.4, 149, 147.1, 145.4, 144.2, 129.8, 127.4, 124.8, 116.5, 112.3, 108.3, 105.1, 100.4, 62.3, 60.9. Anal. calcd. For C₁₉H₁₇NO₅ (339.35): C, 67.25; H, 5.05; N, 4.13; Found: C, 67.45; H, 4.95; N, 4.22.

1-(6-Hydroxy-4,7-dimethoxybenzofuran-5-yl)-3-(p-tolylamino) prop-2-en-1-one (3b). brown oil; yield 40%. The IR (KBr, cm⁻¹) ν 3410 (br, OH and NH), 1701 (C=O). ¹H NMR (300 MHz, DMSO-d₆) δ 12.61 (s, 1H), 10.11 – 10.9 (d, J = 6 Hz, 1H), 8.06 – 8.03 (t, J = 3 Hz, 1H), 7.82 – 7.81 (d, J = 3 Hz, 1H), 7.34 – 7.31 (dd, J = 6, 3 Hz, 2H), 7.23 – 7.20 (dd, 2H), 7.03 – 7.02 (d, J = 3 Hz, 1H), 6.46 - 6.45 (d, J = 3 Hz, 1H), 3.98 (s, 3H, OCH₃), 3.94 (s, 3H, OCH₃), 2.31 (s, 3H, CH₃). ¹³C NMR (75 MHz, DMSO-d₆) δ 181.0 (CO), 154.0, 152.0, 149.5, 146.2, 144.6, 141.3, 132.4, 130.2, 128.0, 118.6, 117.9, 109.1, 106.0, 97.7, 61.9 (OCH₃), 60.0 (OCH₃), 20.6 (CH₃). Anal. calcd. For C₂₀H₁₉NO₅ (353.37): C, 67.98; H, 5.42; N, 3.96; Found: C, 68.08; H, 5.22; N, 4.01.

3-((4-Bromophenyl) amino)-1-(6-hydroxy-4,7-dimethoxybenzo-furan-5-yl) prop-2-en-1-one (3c). brown solid, MP 142-4 °C (MeOH); yield 76%. The IR (KBr, cm⁻¹) ν 3410 (OH), 3120 (NH), 1701 (C=O). ¹H NMR (300 MHz, DMSO-d₆) δ 12.61 (s, 1H), 10.30 - 10.28 (d, J = 6 Hz, 1H), 8.10 – 8.06 (t, J = 6 Hz, 1H), 7.53 – 7.49 (dd, J = 6, 3 Hz, 2H), 7.38 - 7.35 (d, J = 9 Hz,

1H), 7.11 – 7.08 (d, J = 9 Hz, 2H), 6.54 – 6.51 (d, J = 9 Hz, 1H), 6.18 – 6.15 (d, J = 9 Hz, 1H), 3.98 (s, 3H, OCH₃), 3.89 (s, 3H, OCH₃). ¹³C NMR (75 MHz, DMSO-d₆) δ 179.7 (CO), 154.5, 152.6, 149.7, 145.6, 144.6, 142.8, 128.7, 123.2, 117.6, 116.3, 112.1, 108.4, 106, 96.2, 62.7 (OCH₃), 60.3 (OCH₃). Anal. calcd. For C₁₉H₁₆BrNO₅ (418.24): C, 54.56; H, 3.86; Br, 19.10; N, 3.35; Found: C, 54.46; H, 3.76; Br, 19.22; N, 3.44.

3-((4-Chlorophenyl) amino)-1-(6-hydroxy-4,7-dimethoxybenzo-furan-5-yl) prop-2-en-1-one (3d). brown solid, MP 140-2 °C (MeOH); yield 82%. The IR (KBr, cm⁻¹) ν 3420 (OH), 3200 (NH), 1701 (C=O). ¹H NMR (300 MHz, DMSO-d₆) δ 12.63 (s, 1H), 10.30 (d, J = 12.3 Hz, 1H), 8.08 (t, J = 12.6 Hz, 1H), 7.86 (d, J = 2.2 Hz, 1H), 7.42 – 7.34 (m, 2H), 7.17 – 7.11 (m, 2H), 6.53 (d, J = 12.6 Hz, 1H), 6.16 (d, J = 8.1 Hz, 1H), 3.98 (s, 3H, OCH₃), 3.89 (s, 3H, OCH₃). ¹³C NMR (75 MHz, DMSO-d₆) δ 178.9, 152.6, 151.4, 148.7, 146.2, 145.1, 142.8, 128.4, 123.5, 117.9, 115.8, 112.6, 108.7, 106.2, 96.4, 62.1, 61.1. Anal. calcd. For C₁₉H₁₆ClNO₅ (373.79): C, 61.05; H, 4.31; Cl, 9.48; N, 3.75; Found: C, 59.95; H, 4.21; Cl, 9.35; N, 3.66.

3-(Benzyl amino)-1-(6-hydroxy-4,7-dimethoxybenzofuran-5-yl) prop-2-en-1-one (3e): yellow powder, MP 136-8 °C (MeOH); yield 55%. The IR (KBr, cm⁻¹) ν 3450 (OH), 3200 (NH), 1720 (C=O). ¹H NMR (300 MHz, DMSO-d₆) δ 12.67 (s, 1H), 8.59 – 8.57 (d, J = 6 Hz, 1H), 7.89 – 7.87 (d, J = 6 Hz, 1H), 7.65 – 7.59 (t, J = 9 Hz, 1H), 7.39 – 7.24 (m, 5H), 6.93 – 6.90 (d, J = 9 Hz, 1H), 6.62 – 6.60 (d, J = 6 Hz, 1H), 4.48 (s, 2H), 3.90 (s, 3H, OCH₃), 3.87 (s, 3H, OCH₃). ¹³C NMR (75 MHz, DMSO-d₆) δ 188.9, 155.7, 152.7, 149, 145.9, 144.5, 136.7, 129.3, 128.2, 127.5, 126.9, 116.7, 108.2, 105.4, 101.2, 61, 60.2, 53.5. Anal. calcd. For C₂₀H₁₉NO₅ (353.37): C, 67.98; H, 5.42; N, 3.96; Found: C, 68.01; H, 5.32; N, 4.06.

4-((3-(6-Hydroxy-4,7-dimethoxybenzofuran-5-yl)-3-oxoprop-1-en-1-yl) amino) benzene sulfonamide (3f): brown solid, MP 126-8 °C (MeOH); yield 73%. The IR (KBr, cm⁻¹) ν 3450 (br, OH, NH, NH₂), 1707 (C=O). ¹H NMR (300 MHz, DMSO-d₆) δ 12.62 (s, 1H), 11.24 – 11.22 (d, J = 6 Hz, 1H), 7.8 – 7.84 (t, J = 6 Hz, 1H), 7.68 – 7.64 (dd, J = 9, 6 Hz, 2H), 7.57 – 7.56 (d, J = 3 Hz, 1H), 7.33 – 7.29 (dd, J = 9, 3 Hz, 2H), 7.1 (s, 2H), 7.00 – 6.99 (d, J = 3 Hz, 1H), 6.83 – 6.81 (d, J = 6 Hz, 1H), 3.89 (s, 3H, OCH₃), 3.60 (s, 3H, OCH₃). ¹³C NMR (75 MHz, DMSO-d₆) δ 190.6, 152.9, 152.5, 151.3, 146.8, 145.5, 144.5, 135.7, 129.1, 127.6, 119.4, 112.8, 111.0, 108.9, 105.7, 61.6, 61.3. Anal. calcd. For: C₁₉H₁₈N₂O₇S (418.42): C, 54.54; H, 4.34; N, 6.70; S, 7.66; Found: C, 54.35; H, 4.22; N, 6.60; S, 7.86.

N-(4,6-dimethylpyrimidin-2-yl)-4-((3-(6-hydroxy-4,7-dimethoxybenzofuran-5-yl)-3-oxoprop-1-en-1-yl) amino) benzene sulfonamide (3g). brown solid, MP 178-181 °C (MeOH); yield 55%. The IR (KBr, cm⁻¹) ν 3250 (br, OH), 3120 (NH), 1707 (C=O), 1602 (C=N), 1597 (C=C), 1335, 1116 (SO₂NH). ¹H NMR (300 MHz, DMSO-d₆) δ 14.46 (s, 1H), 11.18 (s, 1H), 10.16 (s, 1H), 8.21 – 8.20 (d, J = 3 Hz, 1H), 7.83 – 7.82 (d, J = 3 Hz, 1H), 7.56 – 7.53 (dd, J = 6, 3 Hz, 2H), 7.05 – 7.03 (d, J = 6 Hz, 1H), 6.44 – 6.41 (dd, J = 6, 3 Hz, 2H), 6.19 – 6.18 (d, J = 3 Hz, 1H), 6.13 (s, 1H), 3.93 (s, 3H, OCH₃), 3.86 (s, 3H, OCH₃), 2.04 (s, 6H, 2CH₃). ¹³C NMR (75 MHz, DMSO-d₆) δ 185.7, 167.1, 154.6, 153.2, 151.8, 149.7, 147.1, 145.5, 144.2, 138.5, 128.7, 127.6, 119.2, 116.7, 108.8, 108.1, 105.4, 100.6, 61.0, 60.2, 23.4. Anal. calcd. For: C₂₅H₂₄N₄O₇S (524.55): C, 57.24; H, 4.61; N, 10.68; S, 6.11; Found: C, 57.11; H, 4.45; N, 10.57; S, 6.13.

5-(Benzo [4,5] imidazo[1,2-a] pyrimidin-4-yl)-4,7-dimethoxybenzo-furan-6-ol (3h). brown solid, MP 115-7 °C (MeOH); yield 76%. The IR (KBr, cm⁻¹) ν 3320 (OH), 1707 (C=O), 1620 (C=N), 1567 (C=C). ¹H NMR (300 MHz, DMSO-d₆) δ 14.37 (s, 1H), 7.84 – 7.83 (d, J = 3 Hz, 1H), 7.10 – 7.04 (m, 4H), 6.85 – 6.82 (dd, J = 6, 3 Hz, 2H), 6.09 – 6.07 (d, J = 6 Hz, 1H), 3.94 (s, 3H, OCH₃), 3.86 (s, 3H, OCH₃). ¹³C NMR (75 MHz, DMSO-d₆) δ 156.9, 151.7, 150.2, 149.0, 146.9, 145.9, 143.6, 140.3, 134.7, 129.5, 127.2, 122.8, 117.9, 116.7, 115.5, 113.3, 105.4, 104.1, 61.8, 60.8. Anal. calcd. For: C₂₀H₁₅N₃O₄ (361.36): C, 66.48; H, 4.18; N, 11.63; Found: C, 66.53; H, 4.22; N, 11.45.

6-((3-(6-Hydroxy-4,7-dimethoxybenzofuran-5-yl)-3-oxoprop-1-en-1-yl) amino)-2H-chromen-2-one (3i). yellowish orange crystals, MP 157-9 °C (MeOH); yield 82%. The IR (KBr, cm⁻¹) ν 3320 (OH), 3100 (NH), 1720 (C=O), 1587 (C=C). ¹H NMR (300 MHz, DMSO-d₆) δ 12.97 (s, 1H), 11.10 – 11.08 (d, J = 6 Hz, 1H), 8.07 – 8.05 (d, J = 6 Hz, 1H), 7.98 – 7.96 (d, J = 6 Hz, 1H), 7.73 (s, 1H), 7.43 – 7.39 (t, J = 6 Hz, 1H), 7.37 – 7.34 (dd, J = 6, 3 Hz, 2H), 7.13 – 7.12 (d, J = 3 Hz, 1H), 6.63 – 6.60 (d, J = 9 Hz, 1H), 6.54 – 6.52 (d, J = 6 Hz, 1H), 4.00 (s, 3H, OCH₃), 3.89 (s, 3H, OCH₃). ¹³C NMR (75 MHz, DMSO-d₆) δ 185.4, 161.1, 155.7, 154.6, 152.7, 149.3, 147.1, 144.2, 140.9, 135.7, 127.1, 125.6, 120.5, 119.6, 117.6, 116.3, 115.1, 108.2, 105.4, 100.3, 61.0, 60.2. Anal. calcd. For C₂₂H₁₇NO₇ (407.38): C, 64.86; H, 4.21; N, 3.44; Found: C, 64.92; H, 4.32; N, 3.33.

3-((Furan-2-ylmethyl) amino)-1-(6-hydroxy-4,7-dimethoxy-benzofuran-5-yl) prop-2-en-1-one (3j). yellow crystals, MP 135-7 °C (MeOH); yield 45%. The IR (KBr, cm⁻¹) ν 3300 (OH), 3130 (NH), 1707 (C=O), 1601 (C=C). ¹H NMR (300 MHz, DMSO-d₆) δ 12.42 (s, 1H), 8.49 – 8.47 (d, J = 6 Hz, 1H), 7.57 – 7.56 (d, J = 3 Hz, 1H), 7.42 – 7.36 (t, J = 9 Hz, 1H), 7.29 – 7.28 (d, J = 3 Hz, 1H), 7.00 – 6.99 (d, J = 3 Hz, 1H), 6.67 – 6.64 (d, J = 9 Hz, 1H), 6.30 – 6.27 (dd, J = 6, 3 Hz, 1H), 6.25 – 6.24 (d, J = 3 Hz, 1H), 4.56 (s, 2H), 3.91 (s, 3H, OCH₃), 3.68 (s, 3H, OCH₃). ¹³C NMR (75 MHz, DMSO-d₆) δ 185.7, 153.1, 152.9, 152.5, 151.2, 149.9, 145.5, 141.8, 129.1, 112.7, 111.1, 110.7, 107.2, 105.7, 105.2, 61.5, 61.3, 43.9. Anal. calcd. For C₁₈H₁₇NO₆ (343.34): C, 62.97; H, 4.99; N, 4.08; Found: C, 63.07; H, 5.10; N, 3.9.

General synthesis of compounds 5a-d

A mixture of 2 (22 mg, 10 mmol) and various hydrazonoyl halides (10 mmol) in absolute ethanol (20 mL) and trimethylamine (0.5 mL) was heated under reflux for 3h. The precipitated formed on hot was filtered and recrystallized from ethanol: water (9:1) to afford the corresponding (1H-pyrazol-3-yl) ethan-1-one derivatives **5a-d**.

1-(4-(6-Hydroxy-4,7-dimethoxybenzofuran-5-carbonyl)-1-phenyl-1H-pyrazol-3-yl) ethan-1-one (5a). brown solid, MP 122-5 °C (MeOH); yield 60%. The IR (KBr, cm⁻¹) ν 3400 (OH), 1707, 1698 (C=O), 1620 (C=N), 1578 (C=C). ¹H NMR (300 MHz, DMSO-d₆) δ 14.49 (s, 1H), 8.88 (s, 1H), 7.96 – 7.88 (2d, J = 6, 6, 2H), 7.83 – 7.81 (d, J = 6 Hz, 1H), 7.57 – 7.40 (m, 3H), 7.06 – 7.04 (d, J = 6 Hz, 1H), 3.94 (s, 3H, OCH₃), 3.87 (s, 3H, OCH₃), 2.93 (s, 3H, COCH₃). ¹³C NMR (75 MHz, DMSO-d₆) δ 188.9, 186.4, 156.6, 155.7, 154.6, 147.1, 145.7, 141.3, 136.1, 129.6, 128.7, 127.9, 126.9, 119.5, 117.3, 107.2, 105.2, 61.5, 60.5, 27.8. Anal. calcd. For C₂₂H₁₈N₂O₆ (406.39): C, 65.02; H, 4.46; N, 6.89; Found: C, 64.98; H, 4.55; N, 6.77.

1-(4-(6-Hydroxy-4,7-dimethoxybenzofuran-5-carbonyl)-1-(p-tolyl)-1H-pyrazol-3-yl) ethan-1-one (5b). brown solid, MP 132-4 °C (MeOH); yield 65%. The IR (KBr, cm⁻¹) ν 3300 (OH), 1701 (C=O), 1620 (C=N), 1568 (C=C). ¹H NMR (300 MHz, DMSO-d₆) δ 14.35 (s, 1H), 8.82 (s, 1H), 7.90 – 7.89 (d, J = 3 Hz, 1H), 7.84 – 7.80 (dd, J = 6, 3 Hz, 2H), 7.34 – 7.31 (d, J = 9 Hz, 1H), 7.06 – 7.03 (dd, J = 6, 3 Hz, 2H), 3.94 (s, 3H, OCH₃), 3.86 (s, 3H, OCH₃), 3.19 (s, 3H, COCH₃), 2.35 (s, 3H, CH₃). ¹³C NMR (75 MHz, DMSO-d₆) δ 187.0, 181.2 (CO), 156.4, 156.0, 154.6, 147.1, 143.1, 137.1, 136.7, 132.4, 128.7, 125.6, 118.7, 116.8, 104.6, 95.1, 62.6 (OCH₃), 61.8 (OCH₃), 27.2 (COCH₃), 20.2 (CH₃). Anal. calcd. For C₂₃H₂₀N₂O₆ (420.42): C, 65.71; H, 4.80; N, 6.66; Found: C, 65.66; H, 4.59; N, 6.5.

1-(1-(4-Bromophenyl)-4-(6-hydroxy-4,7-dimethoxybenzofuran-5-carbonyl)-1H-pyrazol-3-yl) ethan-1-one (5c). brown solid, MP 149-153 °C (MeOH); yield 60%. The IR (KBr, cm⁻¹) ν 3310 (OH), 1700, 1654 (C=O), 1601 (C=N), 1568 (C=C). ¹H NMR (300 MHz, DMSO-d₆) δ 12.43 (s, 1H), 8.60 (s, 1H), 7.66 – 7.59 (m, 4H), 7.52 – 7.51 (d, J = 3 Hz, 1H), 7.3 – 7.2 (d, J = 3 Hz, 1H), 3.90 (s, 3H), 3.87 (s, 3H), 2.85 (s, 3H). ¹³C NMR (75 MHz, DMSO-d₆) δ 191.4, 187.8, 155.92, 153.65, 151.24, 147.1, 145.5, 138.5, 132.9, 129.3, 128.6, 123.7, 122.2, 119.7, 113.2, 108.9, 105.7, 61.2, 60.8, 27.8. Anal. calcd. For C₂₂H₁₇BrN₂O₆ (485.29): C, 54.45; H, 3.53; Br, 16.47; N, 5.77; Found: C, 54.35; H, 3.33; Br, 16.51; N, 5.67.

1-(1-(4-Chlorophenyl)-4-(6-hydroxy-4,7-dimethoxybenzofuran-5-carbonyl)-1H-pyrazol-3-yl) ethan-1-one (5d). brown solid, MP 116-8 °C (MeOH); yield 76%. The IR (KBr, cm⁻¹) ν 3350 (OH), 1710, 1698 (C=O), 1620 (C=N), 1598 (C=C). ¹H NMR (300 MHz, DMSO-d₆) δ 14.44 (s, 1H), 8.22 – 8.20 (d, J = 6 Hz, 1H), 8.12 (s, 1H), 7.83 – 8.81 (d, J = 6 Hz, 2H), 7.05 – 7.03 (d, J = 6 Hz, 2H), 6.19 – 6.16 (d, J = 9 Hz, 1H), 3.94 (s, 3H, OCH₃), 3.86 (s, 3H, OCH₃), 2.92 (s, 3H, COCH₃). ¹³C NMR (75 MHz, DMSO-d₆) δ 189.0, 180.4 (CO), 156.0, 154.6, 147.1, 144.2, 141.0, 135.7, 132.6, 131.8, 125.6, 119.6, 117.6, 111.8, 105.4, 96.0, 61.0 (OCH₃), 60.2 (OCH₃), 27.3 (COCH₃). Anal. calcd. For C₂₂H₁₇ClN₂O₆ (440.84): C, 59.94; H, 3.89; Cl, 8.04; N, 6.35; Found: C, 59.86; H, 3.77; Cl, 7.94; N, 6.22.

Antimicrobial assay

In-vitro study

The antimicrobial activity of the synthesized compounds were assessed against *S. aureus* ATCC 6538-P as Gram+ve bacterium, *Escherichia coli* ATCC 25933 as Gram-ve bacterium, *Candida albicans* ATCC 10231 as yeast as well as the filamentous fungal test microbe *Aspergillus niger* NRRL-A326 [44]. Bacterial and yeast test microbes were inoculated on nutrient agar medium plates seeded with 0.1mL of 105-106 cells/mL whereas the fungal test strain was cultivated on plates having potato dextrose agar medium that was seeded by 0.1 mL (106 cells/mL) of the fungal inoculum. 5mg of each sample was dissolved in 2 mL of DMSO. 100 μ l from each sample were distributed in holes developed in each inoculated plate. Then plates were kept at 4 °C for more than 2 hours to allow extreme dispersion. The plates were then kept at 37 °C overnight for bacteria and yeast and kept at 30 °C for 2 days for the fungus in vertical location to permit maximum microbial growth. The clear zone diameters expressed in millimeter (mm) were used to differentiate the antimicrobial activity of tested compounds. The experiment was carried out twice and their mean were considered.

MIC and MBC evaluation

S. aureus ATCC 6538 (Gram positive bacterium), *E. coli* ATCC 25933 (Gram negative bacterium) and *C. albicans* ATCC 10231 (yeast) were cultivated on Mueller Hinton medium. Bacterial cell pellets, collected under sterile condition, were suspended in 20 mL of sterile normal saline with OD of 0.5 to 1.0 giving actual CFU number of about 106 cell/mL. Resazurin solution was prepared (67.5 mg in 10 mL of sterile distilled water) and sterilized by filtration through membrane filter (pore size 0.22 μ m). 100 μ L of the broth culture was dispensed in all wells of the plate then 100 μ L stock concentration of 2.5 mg/mL form each purified compound was pipetted into the first row of the plate and then two-fold dilution has been done up to tenth dilution. 10 μ L of resazurin indicator solution was added to each well and 10 μ L of bacterial suspension (106 cfu/mL) was added to each well. The plates were incubated at 37 °C for 24 h. The colour change was then assessed visually. Any

colour changes from purple to pink or colourless were recorded as positive. The lowest concentration at which colour change occurred was taken as the MIC value [44]. MBC has been performed by streaking of the two concentrations higher than MIC and the plates exhibiting no growth were considered as MBC [44].

DNA gyrase inhibition

E. coli DNA Gyrase inhibition assay was performed using purified *E. coli* DNA gyrase and relaxed DNA kit-plasmid based (TopoGEN) according to manufacturer's instructions. For each reaction we added sterile distilled H₂O, 5x Assay Buffer, pHOT1 Relaxed DNA, about 250 ng of DNA, and *E. coli* DNA gyrase. Then we incubated the reaction mix for 30- 60 min at 37 °C followed by adding 1/5 volume of stop buffer/loading dye. After that we added 20 µL of Chloroform:isoamyl alcohol (24:1 mixture) and vortexed briefly then withdrew the blue aqueous phase. The blue phase was loaded onto a 1% agarose and electrophoresis was conducted until the dye traveled 60-75% down the gel. We stained the gel with 0.5 µg/ml ethidium bromide for 30 min and destained it with distilled water for 10-30 min at room temperature. Finally, we captured the gels images using UV transilluminator [45].

DHFR inhibition

DHFR inhibitor screening kit (BioVision, Catalog #K247-100) was used for this assay [37]. The assay for the inhibitory effect of target compounds against DHFR enzyme was applied as indicated in the DHFR assay kit. DHFR provided with the kit is human DHFR recombinant expressed in *E. coli*. Stock solutions of the tested compounds with different concentrations were prepared by dissolving each tested compounds to 100× in DMSO. Different concentrations (2 µL) of the tested compounds were added into wells of 96-well clear plate. Stock solutions of the DHFR were prepared by adding 2 µL of DHFR to 798 µL of supplied DHFR assay buffer. An amount of 98 µL of diluted DHFR was added into the wells containing the tested samples and enzyme control. An amount of 40 µL of diluted NADPH (10 µL of NADPH in 390 µL DHFR assay buffer) was also added to the aforementioned wells and then mixed well by using vortex. After incubation at room temperature for 10–15 min without exposing to light, 60 µL of diluted DHFR substrate (40 µL of DHFR stock substrate in 560 µL DHFR assay buffer) was added to each well in 96-well plate that contains the test samples and enzyme control and mixed well. Consequently, the total volume is 200 µL. Absorbance was immediately measured at 340 nm in kinetic mode for 10–20 min at room temperature using ELISA reader.

Antioxidant assay

Total antioxidant activity by phosphomolybdenum method.

The total antioxidant capacity (TAC) of the synthesized compounds was evaluated according to the method described by Prieto et al [46]. An aliquot of 100 µL of sample solution was combined with 900 µL of reagent solution (0.6 M sulfuric acid, 28 mM sodium phosphate, and 4 mM ammonium molybdate) (Sigma Aldrich). For the blank, 100 µL of deionized water was used in place of the sample. The tubes were incubated in a boiling water bath at 95 °C for 90 min. After the samples were cooled at room temperature, the absorbance of the aqueous solution of each sample was measured at 695 nm in the spectrophotometer (Shimadzu UV1024-PC). A standard curve of ascorbic acid (0.2-1mg/ml) has been constructed to determine the total antioxidant equivalent at the same time using different concentrations of ascorbic acid (100 – 500 µg/ml). The total antioxidant capacity had been calculated using the following equation based on the calibration curve:

$$y = 0.0036x - 0.2129,$$

where x is the absorbance and y is the ascorbic acid concentration.

DPPH evaluation

The DPPH (2,2- Diphenyl-1-picrylhydrazyl) free radical scavenging capacity of the synthesized analogs was analyzed according to the modified method of Wu et al., 2019 and Ennaji et al, 2020 [47,48]. Each analog was diluted to different concentrations (1000-500-250-125-62.5 and 31.25 µg/mL). 50µL of each analog was added to 1950 µL of 100 µM DPPH ethanol solution (4 mg of PPH in 100 mL methanol). The mixture was shaken vigorously and incubated in dark for 30 min. at room temperature and the absorbance was measured at 517 nm The DPPH scavenging activity was calculated using the following equation:

$$\text{DPPH scavenging activity \%} = \frac{A_0 - A_E}{A_0} \times 100$$

Where A₀ and A_E are the absorbance of the control and compound, respectively.

The IC₅₀ was calculated for each compound. Ascorbic acid was used as standard antioxidant agent.

Molecular docking

Molecular docking study of compounds under investigation together with, **a**: the crystal structure of DNA gyrase B of *S. aureus* (PDB: 2XCT), **b**: the crystal structure of DNA gyrase B of *E. coli* (PDB: 5MMN), and **c**: the crystal structure of DHFR (PDB: 3SQY) of *E. coli* were performed using PyRx tools Autodock Vina (version 1.1.2) [49]. The crystal structures of the previously targets were retrieved from the protein data bank <https://www.rcsb.org>. The native ligands and the water molecules were removed from the proteins using VEGA ZZ 2.3.2 tool followed by adding polar hydrogen and Kollman charges and then converted to PDBQT format by Autodock Vina tools. All designed compounds are saved as a mol file, then protonated, minimized, and converted to pdb file by Open Babel software. The created pdb file was submitted to Autodock Vina tools to

set a few torsions and for pdbqt file construction. AutoGrid was used with a grid box to create the grid map. The number of docked poses generated for each compound was ranked according to the binding energy. The pose of lowest binding energy and 0 Å root-mean-square deviation (RMSD) was considered to be the fittest and most complex with receptor for analysis. The molecular interactions and binding modes of the top poses were visually examined using BIOVIA Discovery Studio 2021.

3. Results and discussion

Synthesis and Characterization

The diverse biological activities linked to the benzofuran scaffold have stimulated additional efforts towards synthesizing different heterocyclic derivatives, motivated by the benzofuran moiety's flexibility. This paper documents the synthesis of various compounds based on a benzofuran-enaminone precursor; a versatile type of precursor that has been documented in very few reports [39,40].

Considering our objective, we report a straightforward coupling procedure, as illustrated in Schemes 1 and 2, that begins with 1-(6-hydroxy-4,7-dimethoxybenzofuran-5-yl) ethane-1-one (**1**). Compound **1** has been synthesized by alkaline hydrolysis of khellin with aqueous sodium hydroxide in water at 100 °C for 45 minutes. Heating of compound **1** with an equal ratio of dimethylformamide-dimethyl acetal (DMF\DMA) under reflux in dry xylene leads to the formation of the corresponding enaminone, 3-(dimethylamino)-1-(6-hydroxy-4,7-dimethoxybenzofuran-5-yl)prop-2-en-1-one (**2**), as reported with sufficient yield 60%.

The reaction of compound **2** with different arylamines including, aniline, p-toluidine, 4-bromoaniline, 4-chloroaniline, benzyl amine in absolute ethanol containing glacial acetic acid (8:2) lead to the formation of the corresponding derivatives of 3-(substituted-amino)-1-(6-hydroxy-4,7-dimethoxybenzofuran-5-yl)prop-2-en-1-ones **3a-e** (Scheme 1, Table 1). In the same manner, compound **2** was reacted with the amino-group of sulfa-drug derivatives (sulfanilamide and sulfadimidine) to give 4-((3-(6-hydroxy-4,7-dimethoxybenzofuran-5-yl)-3-oxoprop-1-en-1-yl) amino) benzene-sulfonamides **3f-g** (Scheme 1). The proposed mechanistic pathway of the reaction of the corresponding enaminone **2** with amine compounds has been done as described by Zuo et al [50].

The chemical structures of the novel derivatives have been verified using elemental analysis and spectral data (IR and NMR). The positions of the functional groups, such as the hydroxyl, carbonyl, and NH groups, were displayed in the IR spectra. In addition to the aromatic protons (H-2 and H-3) of the basic furan moiety, the ¹H NMR analysis of the combined aryl cores revealed further aromatic protons. For example, the IR spectrum of **3c** showed OH at ν 3410, NH at ν 3120, beside the carbonyl group at ν 1701. Its ¹H NMR (DMSO-d₆) spectrum revealed a singlet signal at δ 12.61 attributed to OH in addition to two singlet signals at δ 3.98 and 3.89 confirming the presence of methoxy protons (2 OCH₃). Additionally, two doublet signals at δ 10.30 and 7.38 endorsed the existence of ethylenic protons (CH=CH) besides the doublet signals of H-2 of furan at δ 7.11 and H-3 of furan at δ 6.54. The ¹³C NMR (DMSO-d₆) of **3c** confirmed the presence of carbonyl (CO) at δ 179.7 in addition to the methoxy groups (2 OCH₃) at δ 62.7 and 60.3. For sulfonamide derivatives **3f** and **3g**, the IR spectrum of **3g**, as an example, showed sulfonamide group (SO₂NH) at ν 1335, 1116 besides (OH) and (NH) at ν 3250, 3120, respectively. The ¹H NMR (DMSO-d₆) spectrum of **3g** indicates the presence of two methyl groups of 4,6-dimethylpyrimidine at δ 2.04 as a singlet signal in neighboring to two singlet signals at δ 3.93 and 3.86 attributed to six protons of (2 OCH₃) groups. Additionally, the spectrum confirmed the presence of ethylenic protons (CH=CH) at δ 8.21 and 7.83 besides the doublet signals of H-2 of furan at δ 6.44 and H-3 of furan at δ 6.19.

To enrich the derivatives of 6-hydroxy-4,7-dimethoxybenzofurane, compound **2** has been reacted with some amino-heterocyclic derivatives, namely 2-amino-benzimidazole, 6-amino-coumarin, and furan-2-ylmethanamine under the above conditions (Scheme 1, Table 1). The resulting 6-hydroxy-4,7-dimethoxybenzofurane derivatives **3h-j** have been established based on their elemental analysis and spectral data (IR and NMR). The ¹H NMR (DMSO-d₆) spectrum of **3h** revealed the absence of NH and ethylenic protons and showed the presence of eight aromatic protons, two of them attributed to H-2 and H-3 of furan at δ 6.85 and 6.09, respectively. Besides one singlet signal of OH at δ 14.37, and two singlet signals considering two methoxy protons at δ 3.94 and 3.86. These facts confirmed the formation of benzo [4,5] imidazo[1,2-a] pyrimidine derivative **3h**.

Additionally, to broaden the range of heterocyclic rings that have been hybridized with derivatives of benzofuran, the interaction of enaminone **2** with some of the prepared hydrazone halide derivatives **4a-d** was studied under reflux in absolute ethyl alcohol containing trimethylamine (few drops) to yield the corresponding 1H-pyrazole derivatives **5a-d** (Scheme 2). The proposed mechanism for forming the target benzofuran-containing pyrazole derivatives was depicted in Scheme 2 as described by Zuo et al [50].

IR and NMR spectra, in addition to elemental analysis, were utilized to validate the chemical structures of the resulting 1H-pyrazole derivatives **5a-d**. The ¹H NMR spectra of **5a-d** lacked the presence of ethylenic protons (CH=CH) and revealed new

singlet signals ≈ 2.92 attributed to acetyl protons (COCH₃). Additionally, the ¹³C NMR spectra indicated the presence of the acetyl group at ≈ 27.3 besides the methoxy groups and the aromatic carbons located in their positions. For example, the ¹H NMR spectrum of 5d showed singlet signals at δ 14.44 (OH), 3.94, 3.86 (2 OCH₃), and 2.92 (s, 3H, COCH₃), in addition to doublet signal at δ 6.19 of H-3 of furan. Its ¹³C NMR spectrum revealed signals at δ 27.3 for (COCH₃), 61.0, 60.2 for (2 OCH₃), 189.0 and 180.4 for (2 CO).

Scheme 1. The reaction of enaminone **2** with various amines.

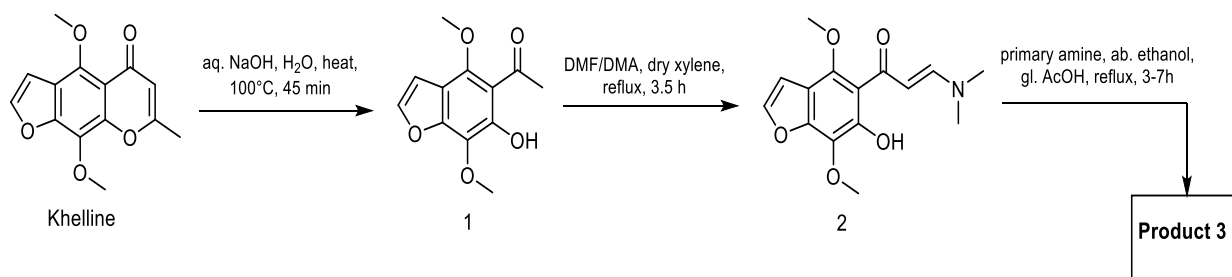
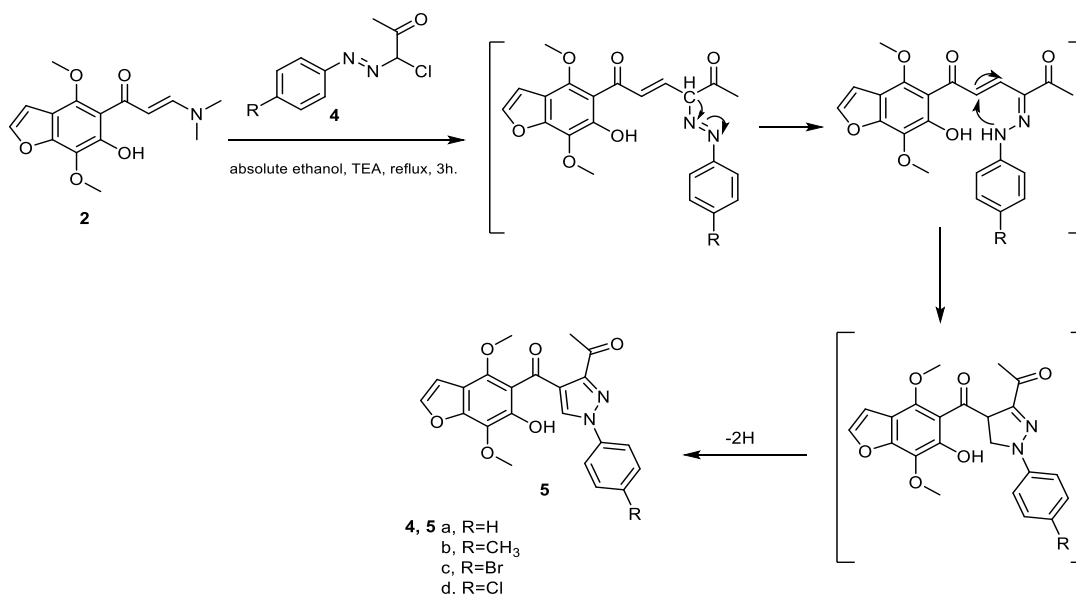


Table 1. Structures of compounds **3a-j**

Compd. No	Reactant amine	Product 3	Compd. No	Reactant amine	Product 3
3a			3f		
3b			3g		
3c			3h		
3d			3i		
3e			3j		

Scheme 2. The reaction of enaminone **2** with some hydrazonyl halide.

Biological activity evaluation

Antimicrobial activity

Using the traditional cup agar plate diffusion method, the newly synthesized enaminone-based benzofuran derivatives **3a-g** and **5a-d** were assessed for their efficacy as antimicrobial agents against *S. aureus* ATCC 6538, *E. coli* ATCC 25922, *C. albicans* ATCC 10231, and *A. niger* NRRL A-326 [44].

Results in Table 2 demonstrated that while compounds **3a** and **3b** had low activities against *S. aureus*, with inhibition zones of 16 and 15 mm, respectively, compounds **3c**, **3d**, **3e**, **3f**, **3h**, **3i**, **5c**, and **5d** did not exhibit anti-Gram-positive activity against *S. aureus*. However, compounds **5a**, **5b**, **3g**, and **3j** showed strong antibacterial activity against *S. aureus* (26, 20, 24, and 21 mm, respectively). Compounds **3a**, **5c**, **5d**, **3h** did not exhibit anti-Gram-negative activity against *E. coli*. The anti-Gram-negative activities of compounds **3b**, **3e**, **3f**, **3i**, **3j**, and **5a** were low, with inhibition zones of 14, 12, 13, 16, 12, and 11 mm, respectively. Compound **3g** was the only one with strong anti-Gram-negative activity (19 mm). Compounds **3b**, **3h**, **3i**, **3j**, **5c**, and **5d** displayed low activities against the yeast test strain (*C. albicans*) with inhibition values of 12, 12, 12, 15, 14, and 13mm, respectively. In contrast, compounds **3a**, **3c**, **3d**, **3f**, **5a**, and **5b** showed no activity against the same test microbe.

Once more, only compound **3g** exhibited potent anti-*C. albicans* activity (29 mm). None of the fourteen compounds exhibited any antifungal action.

Table 2. *In vitro* antimicrobial activity of the active compounds against Gram positive bacterium (*S. aureus*), Gram negative bacterium (*E. coli*), Yeast (*C. albicans*) and fungi (*A. niger*) using agar well diffusion method at concentration (250 µg/100µL)

Compd. No	Inhibition Zone (φmm)			
	<i>S. aureus</i> ATCC 6538	<i>E. coli</i> ATCC 25922	<i>C. albicans</i> ATCC 10231	<i>A. niger</i> NRRL A-326
3a	16	0	0	0
3b	15	14	12	0
3c	0	0	0	0
3d	0	0	0	0
3e	0	12	0	0
3f	0	13	0	0
3g	26	19	29	0
3h	0	0	12	0
3i	0	16	12	0
3j	20	12	15	0
5a	24	11	0	0
5b	21	0	0	0
5c	0	0	14	0
5d	0	0	13	0
neomycin	28	23	26	0
cycloheximide	0	0	0	28

The most potent compounds, namely compounds **3g**, **3j**, **5a** and **5b**, were evaluated for MIC (minimum inhibitory concentration) and MBC (minimum bactericidal concentration) on three different strains, where they showed some promising antimicrobial activities (Table 3).

Table 3. The minimum inhibitory concentrations (MICs, $\mu\text{g/mL}$), and minimum bactericidal concentrations (MBCs, $\mu\text{g/mL}$) of compounds **3g**, **3j**, **5a** and **5b**

Compd No	Pathogenic microorganisms					
	<i>S. aureus</i> ATCC 6538		<i>E. coli</i> ATCC 25922		<i>C. albicans</i> ATCC 10231	
	MIC	MBC	MIC	MBC	MIC	MBC
3g	78.125	312.25	156.25	625	156.25	156.25
3j	312.5	312.5	156.25	312.5	156.25	312.5
5a	156.25	312.5	156.25	156.25	312.5	625
5b	39.06	78.125	78.12	156.25	78.125	312.5
neomycin	39.06	78.125	78.12	156.25	78.125	312.5

Compound **5b** was equipotent with neomycin control drug against all tested stains, *S. aureus*, *E. coli* and *C. albicans* in terms of MIC and MBC values. On the other hand, compound **3g** was 2-fold less potent than neomycin against all strains in terms of MIC, while for MBC it ranged 2-fold more potent in case of *C. albicans*, to 4-fold less potent in case of *S. aureus* and *E. coli*.

Collectively, compounds **3j** and **5a** showed lower antimicrobial activities than **5b** and **3g** against the tested strains. For **3j**, it presented exceptionally low MIC activity against *S. aureus* (8-fold less potent than neomycin) but was only 2-fold less potent than neomycin in case of *E. coli* and *C. albicans*. For MBC values, **3j** ranged from same potency in *C. albicans*, to 2-fold less potent in *E. coli*, to 4-fold less potent in *S. aureus*. Finally, **5a** was 2-fold less potent in terms of MIC against *E. coli*, and 4-fold less potent than neomycin in case of both *S. aureus* and *C. albicans*. MBC values ranged from equipotent to neomycin (*E. coli*), to 2-fold less potent (*C. albicans*), to 4-fold less potent (*S. aureus*).

Sulfonamides (SNs) are an important class of synthetic antimicrobial drugs that are used pharmacologically as broad-spectrum treatments for bacterial infections in humans and animals [51]. On the other hand, the benzofuran moiety containing sulfonamide derivative was reported to exhibit antimicrobial activity [52]. Additionally, benzofuran compounds containing pyrazole derivatives were reported to have antibacterial activity [53]. Considering these findings and the structure-activity relationship, compounds **3g** and **5b**, which accommodate benzofuran-containing sulfadimidine and pyrazole moieties respectively, were identified as potent antibacterial agents. Compound **5b**, which contains the electron-donating (CH_3) group at the para position of the *N*-phenyl at the pyrazole ring, was found to be the most powerful antibacterial agent, exhibiting the lowest MIC values and MBCs.

DNA gyrase inhibitory activity

Analogous to nalidixic acid, norfloxacin (NOR) is one of the strongest inhibitors of DNA gyrase. By attaching itself to DNA gyrase and preventing the untwisting necessary for DNA replication, it prevents bacterial DNA replication. Using NOR as a reference control drug, the two most active compounds, **3g** and **5b**, were subjected to an *E. coli* DNA gyrase inhibition experiment. The results are summarized in Figure 1 as IC_{50} in $\mu\text{g/mL}$. Compound **3g** moderately inhibited DNA gyrase ($\text{IC}_{50} = 5.24 \mu\text{g/mL}$), 3-fold less potent than the reference norfloxacin drug ($\text{IC}_{50} = 1.72 \mu\text{g/mL}$), while **5b** weakly inhibited DNA gyrase ($\text{IC}_{50} = 9.76 \mu\text{g/mL}$), almost 6-fold less potent than norfloxacin.

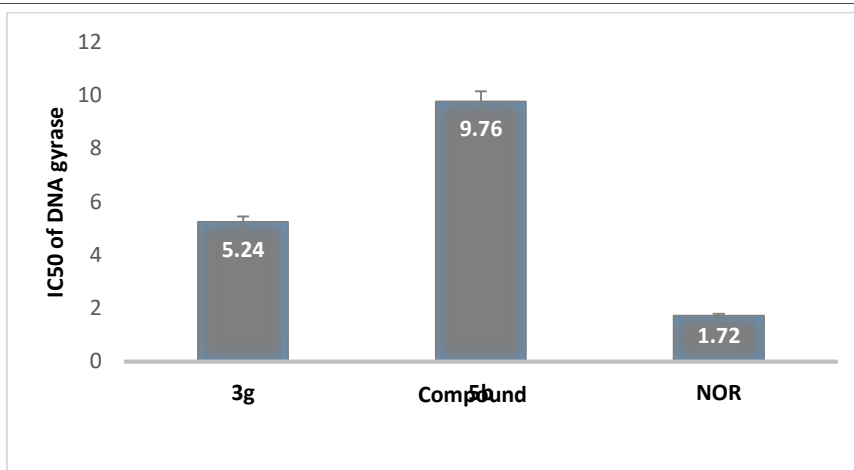


Figure 1. *E. coli* DNA gyrase inhibition results for the two most active compounds **3g** and **5b** using norfloxacin (NOR) as a reference control compound.

DHFR inhibitory activity

An essential component of the metabolism of folate is the enzyme dihydrofolate reductase (DHFR), which is found in all cells. Outcomes of DHFR inhibition include a decrease in intracellular tetrahydrofolate levels, and an inhibition of DNA and RNA synthesis, resulting in cell death. The DHFR inhibitor that has been studied the most is methotrexate (MTX). The purpose of the DHFR inhibition assay is to find DHFR inhibitors. Potential inhibitors are thought to stop the drop in absorbance at an optical density (OD) of 340 nm, which is how DHFR activity is measured. Drug resistance linked to DHFR has become a significant problem in the management of bacterial infections, which is why the most active compounds in this investigation, **3g** and **5b**, were chosen as possible targets for DHFR. The results are summarized in Figure 2 as IC₅₀ in µg/mL. Both compounds moderately inhibited DHFR in vitro, with **3g** showing better inhibition than **5b** (IC₅₀ = 0.38 and 0.7 µg/mL respectively), compared to MTR reference drug (IC₅₀ = 0.15 µg/mL).

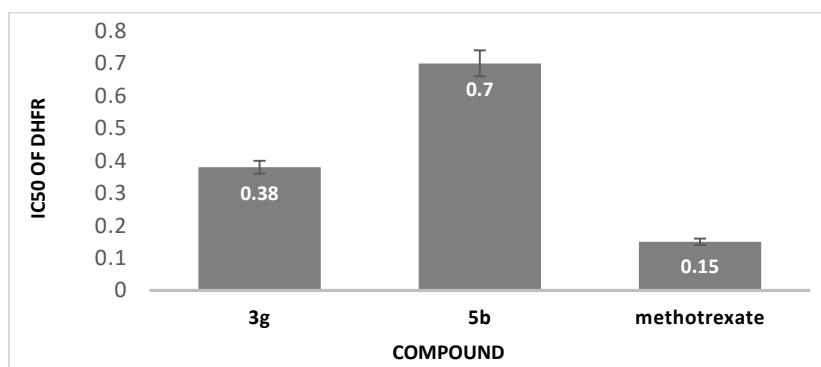


Figure 2. DHFR inhibition results for the two most active compounds **3g** and **5b** using methotrexate as a reference control compound.

Antioxidant activity

Total antioxidant

The antioxidant of the fourteen synthesized compounds had been evaluated using phosphomolybdate method described by Prieto *et al* [46]. It had been evident that all compounds exhibited significant antioxidant activities with values ranging from about 1400 to 1800 µg (ascorbic acid equivalent) AAE/g compound (Table 4). Only compound **3e** exhibited slightly lower antioxidant activity (826.06 µg AAE/g). It had been previously investigated that α,β-unsaturated ketones [54] as well as benzofuran [18] and their derivatives exhibited unique antioxidant activities.

Table 4: The total antioxidant activity of the tested compounds (ascorbic acid equivalent) AAE/g

Compound	Total antioxidant capacity ($\mu\text{g AAE/g}$)
3a	1718.463 \pm 8.684
3b	1622.722 \pm 16.415
3c	1456.981 \pm 12.914
3d	1509.389 \pm 4.444
3e	826.056 \pm 11.824
3f	1663.278 \pm 5.556
3g	1811.426 \pm 1.604
3h	1714.204 \pm 9.787
3i	1672.167 \pm 10.408
3j	1835.315 \pm 7.256
5a	1787.167 \pm 1.667
5b	1826.611 \pm 0.962
5c	1800.5 \pm 2.222
5d	1674.019 \pm 2.245

DPPH scavenging activity

The ability to trap DPPH (2,2- Diphenyl-1-picrylhydrazyl) radicals is detailed for benzofurans derivatives **3g**, **3j**, **5a**, **5b**, and **5c** that showed antioxidant properties in the prior study. Based on how well they can catch both paired and unpaired radicals, antioxidants reduce the absorbance of DPPH radicals by causing an interaction between benzofuran compounds and DPPH radicals that leads to the radical's quest for hydrogen shift. Thus, DPPH is generally utilized as a substrate to assess the anti-oxidative action. Only compounds **5a** and **5b** had an IC_{50} of DPPH scavenging activity almost equal to that of the standard ascorbic acid (Table 5).

Table 5. IC_{50} of DPPH scavenging activities of synthesized compounds **3g**, **3j**, **5a**, **5b**, and **5c** against ascorbic acid (standard compound)

Compd. No.	IC_{50} ($\mu\text{g/mL}$)
3g	597.80 \pm 6.057
3j	659.63 \pm 11.52
5a	414.92 \pm 7.08
5b	435.25 \pm 12.31
5c	723.47 \pm 12.60
Ascorbic acid	410.00 \pm 6.88

Molecular docking studies

To gain a better understanding of the DNA gyrase inhibition and DHFR results, we conducted molecular docking studies of the active compound **3g** with the crystal structures of DNA gyrase B targets in G+ve (PDB: 2XCT) and G-ve (PDB: 5MMN) bacteria as well as DHFR activity in *E. coli* (PDB: 3SQY). We used PyRx tools Autodock Vina (version 1.1.2) for this purpose [49].

The X-ray crystallographic structure of: a, *S. aureus* DNA gyrase B (PDB: 2XCT) with the native ligand (CPF); b, *E. coli* DNA gyrase B (PDB: 5MMN) with the native ligand (O54); and c, *E. coli* DHFR (PDB: 3SQY) with the native ligand (Q11) were downloaded from PDB <https://www.rcsb.org> (log on 27-02-2024). Firstly, the native ligands CPF, O54, and Q11 were re-docked in the enzyme's active cave to ensure the molecular docking technique.

For *S. aureus* DNA gyrase B (PDB: 2XCT), the re-docked CPF recreated the interaction with the basic amino acids (ARG458, SER1085, LYS460, and GLU477) of the active site of DNA gyrase B via hydrogen bonds as reported [55] (Figure 3b).

For *E. coli* DNA gyrase B (PDB: 5MMN), O54 has been connected to the active pocket of DNA gyrase via multi-conventional hydrogen bonds interactions (ASP73, ASN46, ASP49, and VAL43), in addition to π -alkyl interactions with ARG76, GLU50, PRO79, VAL167, VAL71, and ILE94 as reported [56] (Figure 4b).

Regarding to dihydrofolate reductase of *E. coli* (PDB: 3SQY), the Q11 revealed the hydrogen bonds interactions with PHE93, LEU6, and ASP28, besides the π -alkyl interactions with VAL32, ALA8, LEU21, and ILE51 as reported [57] (Figure 5b).

The mode with the lowest binding energy and 0 Å RMSD (root mean square deviation) has been considered the adequate and most complex with the receptor for investigation.

Evaluating the binding mode of the compound 3g with the crystal structures of DNA gyrase B of S. aureus (PDB: 2XCT).

The docking data for **3g** indicate a good binding mode within the active pocket of the DNA gyrase B crystal structure with a binding energy of -5.0 kcal/mol compared to CPF of -3.9 kcal/mol. **3g** interacted with the key amino acids (SER1085,

LYS460, ARG458, and GLU477) of the side chain residue of DNA gyrase B active pocket *via* five hydrogen bonds (Figure 3d).

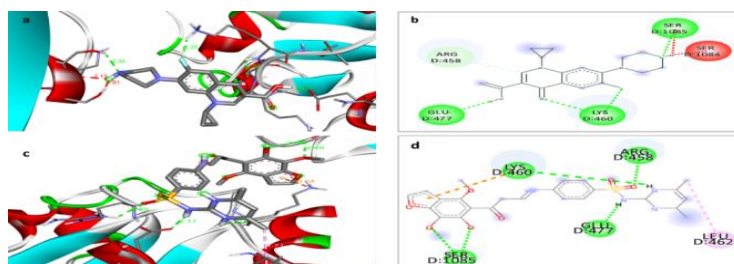


Figure 3 (a & c). The 2D interaction of native ligand CPF and **3g** inside the active pocket of the DNA gyrase of *S. aureus* (PDB: 2XCT).
Figure 3 (b & d). The 3D representations of native ligand CPF and **3g** inside the active pocket of the DNA gyrase of *S. aureus* (PDB: 2XCT).
Evaluating the binding mode of the compound 3g with the crystal structures of DNA gyrase B of E. coli (PDB: 5MMN).

The molecular docking result of **3g** towards DNA gyrase B of *E. coli* (PDB: 5MMN) indicated its good binding mode with a binding energy of -7.8 kcal/mol in comparison with O54 (-9.0 kcal/mol). **3g** formed two hydrogen bonds with ASP73 (key amino acid) and ILE94, in addition to multiple π - interactions with ASP49, VAL71, VAL120, VAL43, ILE78, HIS99, and THR165 (Figure 4d).

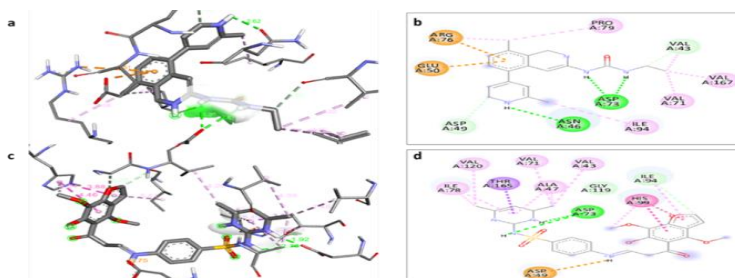


Figure 4 (a & c). The 2D interaction of native ligand O54 and **3g** inside the active pocket of the DNA gyrase of *E. coli* (PDB: 5MMN).
Figure 4 (b & d). The 3D representations of native ligand O54 and **3g** inside the active pocket of the DNA gyrase of *E. coli* (PDB: 5MMN).

Evaluating the binding mode of the compound 3g with the crystal structures of DHFR E. coli (PDB: 3SQY).

3g Demonstrated good binding mode with a binding energy of -5.2 kcal/mol in comparison with Q11 of -8.0 kcal/mol. It showed four hydrogen interactions with TRP23, LEU6, LEU21, and SER50, besides multiple π -interactions with PHE99, LEU29, VAL32, PHE93, and ALA8 (Figure 5d).

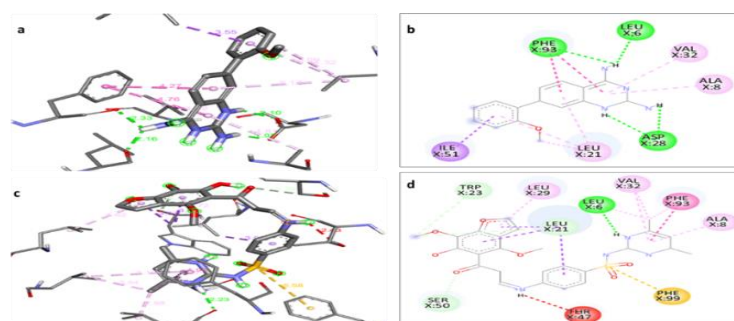


Figure 5 (a & c) the 2D interaction of native ligand Q11 and **3g** inside the active pocket of the DHFR *E. coli* (PDB: 3SQY).
Figure 5 (b & d) the 3D representations of native ligand Q11 and **3g** inside the active pocket of the DHFR *E. coli* (PDB: 3SQY).

Structure activity relationships

Despite the difficulties in finding clear SAR from the biological data, specific conclusions can be extracted:

- Benzofuran derivative **3g** containing a cross-benzofuran-sulfonamide hybrid *via* α , β -unsaturated ketone showed antimicrobial activity against all strains. This confirms the antimicrobial activity of benzofuran bearing sulfonamide, consistent with what has been previously reported [18,52].

- Benzofuran derivative **5b** containing a cross-benzofuran-pyrazole hybrid via carbonyl bridge demonstrated antimicrobial activity equipotent with neomycin control drug against all tested stains, *S. aureus*, *E. coli*, and *C. albicans* in terms of MIC and MBC values. Our data are in alignment with several studies showing the antimicrobial potential of cross-benzofuran-pyrazole hybrid derivatives [58,59].
- Compound **3g** moderately inhibited DNA gyrase ($IC_{50} = 5.24 \mu\text{g} / \text{mL}$), 3-fold less potent than the reference norfloxacin drug ($IC_{50} = 1.72 \mu\text{g} / \text{mL}$). Additionally, **3g** revealed moderate inhibition of DHFR *in vitro* with $IC_{50} = 0.38 \mu\text{g} / \text{mL}$ compared to methotrexate reference drug ($IC_{50} = 0.15 \mu\text{g} / \text{mL}$). The data of DNA gyrase B inhibition activity of **3g** coincides with what was mentioned previously about the importance of benzofuran moiety [60].
- Both benzofuran derivatives **5a** and **5b** revealed antioxidant activity with IC_{50} of DPPH scavenging activity almost equal to that of the standard ascorbic acid, confirming the importance of gathering both benzofuran and pyrazole moieties as previously reported [61,62].

4. Conclusion

Benzofuran derivatives have emerged as a prominent class of compounds in medicinal chemistry due to their diverse biological activities and therapeutic potential. Recently, the synthesis of benzofuran derivatives from enaminones has gained significant attention. This study aims to synthesize a series of novel benzofuran-based enaminones derivatives and evaluate their antimicrobial and antioxidant activities in addition to DNA gyrase and DHFR inhibitory activities. Derivative **3g** containing a cross-benzofuran-sulfonamide hybrid *via* α,β -unsaturated ketone showed antimicrobial activity against all strains, while derivative **5b** containing a cross-benzofuran-pyrazole hybrid *via* carbonyl bridge demonstrated antimicrobial activity equipotent with neomycin control drug against all tested stains in terms of MIC and MBC values. Compound **3g** moderately inhibited DNA gyrase, 3-fold less potent than the reference norfloxacin drug. Additionally, **3g** revealed moderate inhibition of DHFR *in vitro* compared to methotrexate reference drug. Both derivatives **5a** and **5b** revealed antioxidant activity almost equal to that of the standard ascorbic acid, confirming the importance of gathering both benzofuran and pyrazole moieties. Docking studies of compound **3g** on the active sites of DNA gyrase and DHFR confirmed the ability of **3g** to form stable complexes with the target enzymes through hydrogen bonding and hydrophobic interactions. Collectively, compounds **3g** and **5b** showed promising antimicrobial activities, with overall moderate inhibition of DNA gyrase and DHFR. The findings from this research could contribute to the development of new therapeutic agents that address the growing challenges of microbial resistance and oxidative stress-related conditions.

5. Conflicts of Interest

The authors declare no conflicts of interest.

6. Author Contributions

Ashraf A. Sediek: Conceptualization, methodology, interpretation; **Shaima A. El-Mowafi**: methodology, formal analysis, investigation, writing—review and editing; **Eman Sabry**: methodology, investigation. **Mohamed S. Abdel-Aziz**: Conceptualization, methodology, formal analysis, investigation, writing—original draft preparation.

7. Supporting Information

^1H and ^{13}C NMR spectra. This material can be found via the “Supplementary Content” section of this article’s webpage.

8. References

- [1] Sena Murteira Pinheiro, P. de; Franco, L. S.; Montagnoli, T. L.; Fraga, C. A. M. Molecular Hybridization: A Powerful Tool for Multitarget Drug Discovery. *Expert Opin. Drug Discov.* 2024, 19 (4), 451–470. <https://doi.org/10.1080/17460441.2024.2322990>.
- [2] Heba Abdelmohsen; Ahmed M El Kerdawy. "Design, Synthesis, Molecular Docking Studies and in Silico Prediction of ADME Properties of New 5-Nitrobenzimidazole/thiopyrimidine Hybrids as Anti-angiogenic Agents Targeting Hepatocellular Carcinoma". *Egyptian Journal of Chemistry*, 67, 1, 2024, 437-446. doi: 10.21608/ejchem.2023.212212.7998.
- [3] Ashraf A. Sediek; Abeer A. Shaddy; Mohamed A. A. Radwan; Mohamed S. Abdel-aziz. "Design, Synthesis, Anti-Microbial Evaluation, and Docking Studies of New N-Benzyl-3-Indole Derivatives". *Egyptian Journal of Chemistry*, 67, 11, 2024, 57-69. doi: 10.21608/ejchem.2024.304683.10030.
- [4] Viegas-Junior, C.; Danuello, A.; Silva Bolzani, V. da; Barreiro, E. J.; Fraga, C. A. M. Molecular Hybridization: A Useful Tool in the Design of New Drug Prototypes. *Curr. Med. Chem.* 2007, 14 (17), 1829–1852. <https://doi.org/10.2174/092986707781058805>.

- [5] Singh, M.; Sharma, P.; Singh, P. K.; Singh, T. G.; Saini, B. Medicinal Potential of Heterocyclic Compounds from Diverse Natural Sources for the Management of Cancer. *Mini-Rev. Med. Chem.* 2020, 20 (11), 942–957. <https://doi.org/10.2174/1389557520666200212104742>.
- [6] Cheng, Y.; Huang, Z.-T.; Wang, M.-X. Heterocyclic Enamines: The Versatile Intermediates in the Synthesis of Heterocyclic Compounds and Natural Products. *Curr. Org. Chem.* 2004, 8 (4), 325–351. <https://doi.org/10.2174/1385272043485936>.
- [7] Taha A. Hussien; Dina A. El-Amir; Usama A. A. Radwan; Magdi A. El-Sayed; Abou El-Hamd H. Mohamed; Hussein El-Damarany. "Antimicrobial Benzofuran Derivatives and Chemosystematic Significance of *Senecio glaucus* L. (Asteraceae)". *Egyptian Journal of Chemistry*, 66, 10, 2023, 575-583. doi: 10.21608/ejchem.2023.168069.7076.
- [8] Miao, Y.; Hu, Y.; Yang, J.; Liu, T.; Sun, J.; Wang, X. Natural Source, Bioactivity and Synthesis of Benzofuran Derivatives. *RSC Adv* 9 (47), 27510–27540. <https://doi.org/10.1039/c9ra04917g>.
- [9] Heravi, M. M.; Zadsirjan, V.; Hamidi, H.; Amiri, P. H. T. Total Synthesis of Natural Products Containing Benzofuran Rings. *RSC Adv* 2017, 7 (39), 24470–24521. <https://doi.org/10.1039/C7RA03551A>.
- [10] Khalil, N.; Bishr, M.; Desouky, S.; Salama, O. Ammi Visnaga L., a Potential Medicinal Plant: A Review. *Molecules* 2020, 25 (2), 301. <https://doi.org/10.3390/molecules25020301>.
- [11] Radadiya, A.; Shah, A. Bioactive Benzofuran Derivatives: An Insight on Lead Developments, Radioligands and Advances of the Last Decade. *Eur. J. Med. Chem.* 2015, 97, 356–376. <https://doi.org/10.1016/j.ejmech.2015.01.021>.
- [12] Rao, M. L. N.; Murty, V. N. Rapid Access to Benzofuran-Based Natural Products through a Concise Synthetic Strategy. *Eur. J. Org. Chem.* 2016, 2016 (12), 2177–2186. <https://doi.org/10.1002/ejoc.201600154>.
- [13] Khodarahmi, G.; Asadi, P.; Hassanzadeh, F.; Khodarahmi, E. Benzofuran as a Promising Scaffold for the Synthesis of Antimicrobial and Anticancer Agents: A Review. *J. Res. Med. Sci. : The Official Journal of Isfahan University of Medical Sciences* 2015, 20 (11), 1094. <https://doi.org/10.4103/1735-1995.172835>.
- [14] Xu, Z.; Xu, D.; Zhou, W.; Zhang, X. Therapeutic Potential of Naturally Occurring Benzofuran Derivatives and Hybrids of Benzofurans with Other Pharmacophores as Antibacterial Agents. *Curr. Top. Med. Chem.* 2022, 22 (1), 64–82.
- [15] Kenchappa, R.; Bodke, Y. D.; Telkar, S.; Aruna Sindhe, M. Antifungal and Anthelmintic Activity of Novel Benzofuran Derivatives Containing Thiazolo Benzimidazole Nucleus: An in Vitro Evaluation. *J. Chem. Biol.* 2016, 10 (1), 11–23. <https://doi.org/10.1007/s12154-016-0160-x>.
- [16] Masubuchi, M.; Ebiike, H.; Kawasaki, K.; Sogabe, S.; Morikami, K.; Shiratori, Y.; Tsujii, S.; Fujii, T.; Sakata, K.; Hayase, M.; Shindoh, H.; Aoki, Y.; Ohtsuka, T.; Shimma, N. Synthesis and Biological Activities of Benzofuran Antifungal Agents Targeting Fungal N-Myristoyltransferase. *Bioorg. Med. Chem.* 2003, 11 (20), 4463–4478. [https://doi.org/10.1016/S0968-0896\(03\)00429-2](https://doi.org/10.1016/S0968-0896(03)00429-2).
- [17] Xu, Z.; Zhao, S.; Lv, Z.; Feng, L.; Wang, Y.; Zhang, F.; Bai, L.; Deng, J. Benzofuran Derivatives and Their Anti-Tubercular, Anti-Bacterial Activities. *Eur. J. Med. Chem.* 2019, 162, 266–276. <https://doi.org/10.1016/j.ejmech.2018.11.025>.
- [18] Chand, K.; Rajeshwari, null; Hiremathad, A.; Singh, M.; Santos, M. A.; Keri, R. S. A Review on Antioxidant Potential of Bioactive Heterocycle Benzofuran: Natural and Synthetic Derivatives. *Pharmacol Rep.* 2017, 69 (2), 281–295. <https://doi.org/10.1016/j.pharep.2016.11.007>.
- [19] Rindhe, S. S.; Rode, M. A.; Karale, B. K. New Benzofuran Derivatives as an Antioxidant Agent. *Ind. J. Pharm. Sci.* 2010, 72 (2), 231. <https://doi.org/10.4103/0250-474X.65022>.
- [20] Ayoub, A. J.; El-Achkar, G. A.; Ghayad, S. E.; Hariss, L.; Haidar, R. H.; Antar, L. M.; Mallah, Z. I.; Badran, B.; Grée, R.; Hachem, A.; Hamade, E.; Habib, A. Fluorinated Benzofuran and Dihydrobenzofuran as Anti-Inflammatory and Potential Anticancer Agents. *Int. J. Mol. Sci.* 2023, 24 (12), 10399. <https://doi.org/10.3390/ijms241210399>.
- [21] Bodke, R. K.; Synthesis, Y. D. Analgesic and Anti-Inflammatory Activity of Benzofuran Pyrazole Heterocycles. *Chem. Data Collect.* 2020, 28, 100453. <https://doi.org/10.1016/j.cdc.2020.100453>.
- [22] Dawood, K. M.; Abdel-Gawad, H.; Rageb, E. A.; Ellithey, M.; Mohamed, H. A. Synthesis, Anticonvulsant, and Anti-Inflammatory Evaluation of Some New Benzotriazole and Benzofuran-Based Heterocycles. *Bioorg. Med. Chem.* 2006, 14 (11), 3672–3680. <https://doi.org/10.1016/j.bmc.2006.01.033>.
- [23] Abdelrahman, M. A.; Eldehna, W. M.; Nocentini, A.; Ibrahim, H. S.; Almahli, H.; Abdel-Aziz, H. A.; Abou-Seri, S. M.; Supuran, C. T. Novel Benzofuran-Based Sulphonamides as Selective Carbonic Anhydrases IX and XII Inhibitors: Synthesis and in Vitro Biological Evaluation. *J. Enzyme Inhib. Med. Chem.* 35 (1), 298–305. <https://doi.org/10.1080/14756366.2019.1697250>.
- [24] Montanari, S.; Mahmoud, A. M.; Pruccoli, L.; Rabbito, A.; Naldi, M.; Petralla, S.; Moraleda, I.; Bartolini, M.; Monti, B.; Iriepa, I.; Belluti, F.; Gobbi, S.; Di Marzo, V.; Bisi, A.; Tarozzi, A.; Ligresti, A.; Rampa, A. Discovery of Novel Benzofuran-Based Compounds with Neuroprotective and Immunomodulatory Properties for Alzheimer's Disease Treatment. *Eur. J. Med. Chem.* 2019, 178, 243–258. <https://doi.org/10.1016/j.ejmech.2019.05.080>.
- [25] Riyahi, Z.; Asadi, P.; Hassanzadeh, F.; Khodamoradi, E.; Gonzalez, A.; Karimi Abdolmaleki, M. Synthesis of Novel Conjugated Benzofuran-Triazine Derivatives: Antimicrobial and in-Silico Molecular Docking Studies. *Heliyon* 2023, 9 (8), e18759. <https://doi.org/10.1016/j.heliyon.2023.e18759>.
- [26] El-Sawy, E. R.; Shaker, K. H.; Mandour, A. H.; Shehab El-Din, A.; Abdula, M. M. Synthesis and Pharmacological Activities of Novel Furobenzopyrone and Benzofuran Derivatives. *Ind. J. Chem. - Section B Org. and Med. Chem.* 2008, 47 (9), 1451–1462.
- [27] El-Shihi, T. H.; Abdel Latif, N. A.; El-Sawy, E. R. Synthesis of Some New Benzofuran Derivatives as Photochemical Probe in Biological System. *Egypt. J. Chem.* 2005, 48 (3), 365–376.
- [28] El-Sawy, E. R.; Ebaid, M. S.; Abo-Salem, H. M.; Al-Sehemi, A. G.; Mandour, A. H. Synthesis, Anti-Inflammatory, Analgesic and Anticonvulsant Activities of Some New 4,6-Dimethoxy-5-(Heterocycles)Benzofuran Starting from Naturally Occurring Visnagin. *Arab. J. Chem.* 2014, 7 (6), 914–923. <https://doi.org/10.1016/j.arabjc.2012.12.041>.

- [29] Dawood, K. An Update on Benzofuran Inhibitors: A Patent Review. *Expert Opin. Ther. Patents* 2019, 29. <https://doi.org/10.1080/13543776.2019.1673727>.
- [30] Abbas, A. A.; Dawood, K. M. Anticancer Therapeutic Potential of Benzofuran Scaffolds. *RSC Adv.* 2023, 13 (16), 11096–11120. <https://doi.org/10.1039/D3RA01383A>.
- [31] Farhat, J.; Alzyoud, L.; Alwahsh, M.; Al-Omari, B. Structure–Activity Relationship of Benzofuran Derivatives with Potential Anticancer Activity. *Cancers* 2022, 14 (9), 2196. <https://doi.org/10.3390/cancers14092196>.
- [32] Ma, Y.; Zheng, X.; Gao, H.; Wan, C.; Rao, G.; Mao, Z. Design, Synthesis, and Biological Evaluation of Novel Benzofuran Derivatives Bearing N-Aryl Piperazine Moiety. *Molecules* 2016, 21 (12), 1684. <https://doi.org/10.3390/molecules21121684>.
- [33] Murray, C. J. L.; Ikuta, K. S.; Sharara, F.; Swetschinski, L.; Aguilar, G. R.; Gray, A.; Han, C.; Bisignano, C.; Rao, P.; Wool, E.; Johnson, S. C.; Browne, A. J.; Chipeta, M. G.; Fell, F.; Hackett, S.; Haines-Woodhouse, G.; Hamadani, B. H. K.; Kumaran, E. A. P.; McManigal, B.; Achalapong, S.; Agarwal, R.; Akech, S.; Albertson, S.; Amuasi, J.; Andrews, J.; Aravkin, A.; Ashley, E.; Babin, F.-X.; Bailey, F.; Baker, S.; Basnyat, B.; Bekker, A.; Bender, R.; Berkley, J. A.; Bethou, A.; Bielicki, J.; Boonkasidecha, S.; Bukosia, J.; Carvalheiro, C.; Castañeda-Orjuela, C.; Chansamouth, V.; Chaurasia, S.; Chiurchiù, S.; Chowdhury, F.; Donatien, R. C.; Cook, A. J.; Cooper, B.; Cressey, T. R.; Criollo-Mora, E.; Cunningham, M.; Darboe, S.; Day, N. P. J.; Luca, M. D.; Dokova, K.; Dramowski, A.; Dunachie, S. J.; Bich, T. D.; Eckmanns, T.; Eibach, D.; Emami, A.; Feasey, N.; Fisher-Pearson, N.; Forrest, K.; Garcia, C.; Garrett, D.; Gastmeier, P.; Giref, A. Z.; Greer, R. C.; Gupta, V.; Haller, S.; Haselbeck, A.; Hay, S. I.; Holm, M.; Hopkins, S.; Hsia, Y.; Ireghu, K. C.; Jacobs, J.; Jarovsky, D.; Javanmardi, F.; Jenney, A. W. J.; Khorana, M.; Khusuwan, S.; Kissoon, N.; Kobeissi, E.; Kostyanev, T.; Krapp, F.; Krumkamp, R.; Kumar, A.; Kyu, H. H.; Lim, C.; Lim, K.; Limmathurotsakul, D.; Loftus, M. J.; Lunn, M.; Ma, J.; Manoharan, A.; Marks, F.; May, J.; Mayxay, M.; Mturi, N.; Munera-Huertas, T.; Musicha, P.; Musila, L. A.; Mussi-Pinhata, M. M.; Naidu, R. N.; Nakamura, T.; Nanavati, R.; Nangia, S.; Newton, P.; Ngoun, C.; Novotney, A.; Nwakanma, D.; Obiero, C. W.; Ochoa, T. J.; Olivás-Martínez, A.; Olliaro, P.; Ooko, E.; Ortiz-Brizuela, E.; Ounchanum, P.; Pak, G. D.; Paredes, J. L.; Peleg, A. Y.; Perrone, C.; Phe, T.; Phommason, K.; Plakkal, N.; Ponce-de-Leon, A.; Raad, M.; Ramdin, T.; Rattanavong, S.; Riddell, A.; Roberts, T.; Robotham, J. V.; Roca, A.; Rosenthal, V. D.; Rudd, K. E.; Russell, N.; Sader, H. S.; Saengchan, W.; Schnall, J.; Scott, J. A. G.; Seekaew, S.; Sharland, M.; Shivamallappa, M.; Sifuentes-Osornio, J.; Simpson, A. J.; Steenkeste, N.; Stewardson, A. J.; Stoeva, T.; Tasak, N.; Thaiprakong, A.; Thwaites, G.; Tigoï, C.; Turner, C.; Turner, P.; Doorn, H. R. van; Velaphi, S.; Vongpradith, A.; Vongsouvath, M.; Vu, H.; Walsh, T.; Walson, J. L.; Waner, S.; Wangrangsimakul, T.; Wannapinij, P.; Wozniak, T.; Sharma, T. E. M. W. Y.; Yu, K. C.; Zheng, P.; Sartorius, B.; Lopez, A. D.; Stergachis, A.; Moore, C.; Dolecek, C.; Naghavi, M. Global Burden of Bacterial Antimicrobial Resistance in 2019: A Systematic Analysis. *The Lancet* 2022, 399 (10325), 629–655. [https://doi.org/10.1016/S0140-6736\(21\)02724-0](https://doi.org/10.1016/S0140-6736(21)02724-0).
- [34] Eijk, E. van; Wittekoek, B.; Kuijper, E. J.; Smits, W. K. DNA Replication Proteins as Potential Targets for Antimicrobials in Drug-Resistant Bacterial Pathogens. *J. Antimicrob. Chemother* 2017, 72 (5), 1275–1284. <https://doi.org/10.1093/jac/dkw548>.
- [35] Marchese, A.; Debbia, E. A. The Role of *gyrA*, *gyrB*, and *dnaA* Functions in Bacterial Conjugation. *Ann. Microbiol.* 2016, 66 (1), 223–228. <https://doi.org/10.1007/s13213-015-1098-x>.
- [36] Dighe, S. N.; Collet, T. A. Recent Advances in DNA Gyrase-Targeted Antimicrobial Agents. *European J. Med. Chem.* 2020, 199, 112326. <https://doi.org/10.1016/j.ejmech.2020.112326>.
- [37] Ghany, L. M. A. A.; Ryad, N.; Abdel-Aziz, M. S.; El-Lateef, H. M. A.; Zaki, I.; Beshay, B. Y. Design, Synthesis, Antimicrobial Evaluation, and Molecular Modeling of New Sulfamethoxazole and Trimethoprim Analogs as Potential DHPS/DHFR Inhibitors. *J. Mol. Struct.* 2024, 138170. <https://doi.org/10.1016/j.molstruc.2024.138170>.
- [38] Hiremathad, A.; Patil, M. R.; R, C. K.; Chand, K.; Santos, M. A.; Keri, R. S. Benzofuran: An Emerging Scaffold for Antimicrobial Agents. *RSC Adv.* 2015, 5 (117), 96809–96828. <https://doi.org/10.1039/C5RA20658H>.
- [39] Sanad, S. M. H.; Mekky, A. E. M. Enaminone Incorporating a Dibromobenzofuran Moiety: Versatile Precursor for Novel Azines and Azolotriazines. *J. Het. Chem.* 2018, 55 (4), 836–843. <https://doi.org/10.1002/jhet.3107>.
- [40] Ahmed, A. A. M.; Mekky, A. E. M.; Sanad, S. M. H. New Piperazine-Based Bis(Thieno[2,3-b]Pyridine) and Bis(Pyrazolo[3,4-b]Pyridine) Hybrids Linked to Benzofuran Units: Synthesis and in Vitro Screening of Potential Acetylcholinesterase Inhibitors. *Synth. Commun.* 2022, 52 (6), 912–925. <https://doi.org/10.1080/00397911.2022.2056853>.
- [41] Schönberg, A.; Sina, A. Khellin and Allied Compounds. *J. Am. Chem. Soc.* 1950, 72 (4), 1611–1616. <https://doi.org/10.1021/ja01160a051>.
- [42] Gammill, R. B.; Day, C. E.; Schurr, P. E. Khellin Analogs. 1. General Topological Requirements for Lipid-Altering Activity in Furochromones. *J. Med. Chem.* 1983, 26 (12), 1672–1674. <https://doi.org/10.1021/jm00366a002>.
- [43] Löwe, W.; Müller, B. Norkhellin-Derivate Mit Schwefelfunktionen. *Arch. Pharm.* 1986, 319 (3), 252–255. <https://doi.org/10.1002/ardp.19863190311>.
- [44] Abo-Salem, H. M.; Abd El Salam, H. A.; Abdel-Aziem, A.; Abdel-Aziz, M. S.; El-Sawy, E. R. Synthesis, Molecular Docking, and Biofilm Formation Inhibitory Activity of Bis(Indolyl)Pyridines Analogues of the Marine Alkaloid Nortopsentin. *Molecules* 2021, 26 (14), 4112. <https://doi.org/10.3390/molecules26144112>.
- [45] Mora-Pale, M.; Bhan, N.; Masuko, S.; James, P.; Wood, J.; McCallum, S.; Linhardt, R. J.; Dordick, J. S.; Koffas, M. A. G. Antimicrobial Mechanism of Resveratrol-Trans-Dihydrodimer Produced from Peroxidase-Catalyzed Oxidation of Resveratrol. *Biotechnol. Bioeng.* 2015, 112 (12), 2417–2428. <https://doi.org/10.1002/bit.25686>.
- [46] Prieto, P.; Pineda, M.; Aguilar, M. Spectrophotometric Quantitation of Antioxidant Capacity through the Formation of a Phosphomolybdenum Complex: Specific Application to the Determination of Vitamin E. *Anal. Biochem.* 1999, 269 (2), 337–341. <https://doi.org/10.1006/abio.1999.4019>.

- [47] Wu, Z.; Tan, B.; Liu, Y.; Dunn, J.; Martorell Guerola, P.; Tortajada, M.; Cao, Z.; Ji, P. Chemical Composition and Antioxidant Properties of Essential Oils from Peppermint, Native Spearmint and Scotch Spearmint. *Molecules* 2019, 24 (15), 2825. <https://doi.org/10.3390/molecules24152825>.
- [48] Ennaji, H.; Chahid, D.; Aitssi, S.; Badou, A.; Khilil, N.; Ibenmoussa, S.; Ennaji, H.; Chahid, D.; Aitssi, S.; Badou, A.; Khilil, N.; Ibenmoussa, S. Phytochemicals Screening, Cytotoxicity and Antioxidant Activity of the *Origanum Majorana* Growing in Casablanca, Morocco. *Open J. Bio. Sci.* 2020, 5 (1), 053–059. <https://doi.org/10.17352/ojbs.000026>.
- [49] Dallakyan, S.; Olson, A. J. Small-Molecule Library Screening by Docking with PyRx. *Methods Mol. Biol.* 2015, 1263, 243–250. https://doi.org/10.1007/978-1-4939-2269-7_19.
- [50] Zuo, W.; Zuo, L.; Geng, X.; Li, Z.; Wang, L. Radical-Polar Crossover Enabled Triple Cleavage of CF₂Br₂: A Multicomponent Tandem Cyclization to 3-Fluoropyrazoles. *Org. Lett.* 2023, 25 (32), 6062–6066. <https://doi.org/10.1021/acs.orglett.3c02305>.
- [51] Ovung, A.; Bhattacharyya, J. Sulfonamide Drugs: Structure, Antibacterial Property, Toxicity, and Biophysical Interactions. *Biophys. Rev.* 2021, 13 (2), 259–272. <https://doi.org/10.1007/s12551-021-00795-9>.
- [52] Venkateswarlu, T.; Anisetti, R. N.; Rao, R.; Ram, B.; Balram, B. Synthesis and Antimicrobial Activity of Novel Benzo[b]Furan Derivatives Bearing Sulphonamide and Phenylcarbamate Moieties. *Der Pharmacia Sinica* 2014, 5, 101–105.
- [53] Elsharif, M.; Hassan, A.; Moustafa, G.; Awad, H.; Mohamed, N. Antimicrobial Evaluation and Molecular Properties Prediction of Pyrazolines Incorporating Benzofuran and Pyrazole Moieties ARTICLE INFO. *J. App. Pharm. Sci.* 2020, 10, 37–043. <https://doi.org/10.7324/JAPS.2020.102006>.
- [54] Okolo, E. N.; Ugwu, D. I.; Ezema, B. E.; Ndefo, J. C.; Eze, F. U.; Ezema, C. G.; Ezugwu, J. A.; Ujam, O. T. New Chalcone Derivatives as Potential Antimicrobial and Antioxidant Agent. *Sci. Rep.* 2021, 11 (1), 21781. <https://doi.org/10.1038/s41598-021-01292-5>.
- [55] Patel, M. M.; Patel, L. J. Design, Synthesis, Molecular Docking, and Antibacterial Evaluation of Some Novel Flouroquinolone Derivatives as Potent Antibacterial Agent. *Sci. World J.* 2014, 2014, 897187. <https://doi.org/10.1155/2014/897187>.
- [56] Elghareeb, F. H.; Kandil, E. M.; Abou-Elzahab, M.; Abdelmoteleb, M.; Abozeid, M. A. Rigid 3D-Spiro Chromanone as a Crux for Efficient Antimicrobial Agents: Synthesis, Biological and Computational Evaluation. *RSC Adv.* 2021, 11 (35), 21301–21314. <https://doi.org/10.1039/D1RA03497A>.
- [57] Li, X.; Hilgers, M.; Cunningham, M.; Chen, Z.; Trzoss, M.; Zhang, J.; Kohnen, L.; Lam, T.; Creighton, C.; Gc, K.; Nelson, K.; Kwan, B.; Stidham, M.; Brown-Driver, V.; Shaw, K. J.; Finn, J. Structure-Based Design of New DHFR-Based Antibacterial Agents: 7-Aryl-2,4-Diaminoquinazolines. *Bioorg. Med. Chem. Lett.* 2011, 21 (18), 5171–5176. <https://doi.org/10.1016/j.bmcl.2011.07.059>.
- [58] Sanad, S. M. H.; Hanna, D. H.; Mekky, A. E. M. Regioselective Synthesis of Novel Antibacterial Pyrazole-Benzofuran Hybrids: 2D NMR Spectroscopy Studies and Molecular Docking. *J. Mol. Struct.* 2019, 1188, 214–226. <https://doi.org/10.1016/j.molstruc.2019.03.088>.
- [59] A Alam, M. Antibacterial Pyrazoles: Tackling Resistant Bacteria. *Future Med. Chem.* 2022, 14 (5), 343–362. <https://doi.org/10.4155/fmc-2021-0275>.
- [60] Kummetha, I.; Konduri, S.; Janupally, R.; Sree, K.; Chuppala, A.; Jeankumar, V.; Sridevi, J.; Babu, K.; Perumal, Y.; Sriram, D. An Efficient Synthesis and Biological Screening of Benzofuran and Benzo[d]Isothiazole Derivatives for Mycobacterium Tuberculosis DNA GyrB Inhibition. *Bioorg. Med. Chem.* 2014, 22. <https://doi.org/10.1016/j.bmc.2014.10.016>.
- [61] Rangaswamy, J.; Vijay Kumar, H.; Harini, S. T.; Naik, N. Synthesis of Benzofuran Based 1,3,5-Substituted Pyrazole Derivatives: As a New Class of Potent Antioxidants and Antimicrobials-A Novel Accost to Amend Biocompatibility. *Bioorg. Med. Chem. Lett.* 2012, 22 (14), 4773–4777. <https://doi.org/10.1016/j.bmcl.2012.05.061>.
- [62] Rangaswamy, J.; Kumar, H. V.; Harini, S. T.; Naik, N. Functionalized 3-(Benzofuran-2-Yl)-5-(4-Methoxyphenyl)-4,5-Dihydro-1H-Pyrazole Scaffolds: A New Class of Antimicrobials and Antioxidants. *Arab. J. Chem.* 2017, 10, S2685–S2696. <https://doi.org/10.1016/j.arabjc.2013.10.012>.